

Article

Multiple Extended Target Tracking Algorithm Based on Spatio-Temporal Correlation

Wei Zhang ^{1,*}, Chen Lin ², Tingting Liu ¹ and Lu Gan ^{2,3}

¹ National Key Laboratory of Electromagnetic Space Security, Jiaxing 314000, China; ltt18257339581@163.com

² Information and Communication Engineering, University of Electronic Science and Technology of China (UESTC), Chengdu 611731, China; jeremylinpp@163.com (C.L.); ganlu@uestc.edu.cn (L.G.)

³ Yibin Research Institute of University of Electronic Science and Technology of China, Yibin 643000, China

* Correspondence: zwlab36@163.com

Abstract: In the clutter environment, the measurement of a set of multiple extended targets, with an unknown number of targets, poses challenges in partitioning, and the computational cost is high. In particular, the multiple extended target tracking method, based on distance partition, has obvious potential estimation errors when the extended targets intersect. This paper proposes a partition algorithm, based on spatio-temporal correlation, which considers the correlation between adjacent moments of the extended target and uses this prior information to divide the measurement set into a survival target measurement set and a born target measurement set for the first time. Then, the survival target measurement set is clustered by the K-means++ algorithm, and the extended target tracking is transformed into point target tracking. The born target measurement undergoes preprocessing by the DBSCAN clustering algorithm, and then uses the directed graph with shared nearest neighbors (SNN) dividing the measurement set. The method proposed in this paper significantly reduces the number of partitions and the computational time. The effectiveness of the algorithm is demonstrated through experimental simulations.

Keywords: multi-extended target tracking; spatio-temporal correlation; measurement set partition; probability hypothesis density filter



Citation: Zhang, W.; Lin, C.; Liu, T.; Gan, L. Multiple Extended Target Tracking Algorithm Based on Spatio-Temporal Correlation. *Appl. Sci.* **2024**, *14*, 2367. <https://doi.org/10.3390/app14062367>

Academic Editor: Amerigo Capria

Received: 29 January 2024

Revised: 7 March 2024

Accepted: 8 March 2024

Published: 11 March 2024



Copyright: © 2024 by the authors. Licensee MDPI, Basel, Switzerland. This article is an open access article distributed under the terms and conditions of the Creative Commons Attribution (CC BY) license (<https://creativecommons.org/licenses/by/4.0/>).

1. Introduction

In the traditional multi-target tracking (MTT) [1] scenario, a single target generates, at most, one measurement at a time. In this case, the target can be regarded as a point target and its shape can be ignored. However, with the development of modern high-resolution sensors, the target will occupy multiple resolution cells of the sensor, so the point target model is no longer applicable. Instead, the target should be modeled as an extended target (ET), where a single target generates multiple measurements at each time.

In the past few years, the extended target tracking problem has attracted a lot of attention; the references [2,3] summarize the extended target tracking problem. At present, the measurement model of the extended target is mostly based on the non-uniform Poisson process measurement model proposed by Gilholm and Salmond [4], which assumes that the measurement sources of the extended target are randomly distributed around the center of mass of the extended target, and the measurements received by sensors about the target and clutter at the same time all follow Poisson distribution. The extended target cannot be modeled by the point target model, and its shape model should be considered. At present, the modeling methods of extended target shape mainly include random matrix (RM) [5,6], random hypersurface model (RHM) [7], and Gaussian process (GP) [8]. The RM method assumes that the shape of the target is approximately an ellipse, while the RHM and GP methods no longer limit the shape of the target to an ellipse, but a more irregular shape; however, these two modeling methods also result in more computational complexity.

In recent years, the extended target tracking method based on random finite set (RFS) has received extensive attention. Since the target tracking framework based on RFS has a strict Bayesian theory foundation, it can simultaneously estimate the number of targets and the state without considering the data association. Therefore, it is particularly suitable for multiple extended target tracking problems. The RFS framework for MTT proposed by Mahler [9], driven by the inherent combinatorial characteristics of Bayesian multi-objective filters, has led to the utilization of probability hypothesis density (PHD) [10], cardinalized PHD (CPHD) [11], and multi-Bernoulli filters [12,13] to approximate optimal Bayesian filtering. Based on the extended target Poisson model proposed by Gilholm, Mahler derived the measurement update equation of the PHD filter. However, the measurement update equation remains intractable.

Granstrom proposed a tractable extended target Gaussian mixture PHD filter algorithm (ET-GM-PHD) [14], and proposed a distance partition (DP) method to partition the measurement set. The Gaussian-inverse-Wishart PHD (GIW-PHD) filtering algorithm [6], which combines RM with the ET-PHD framework, can not only estimate the motion state of the target, but also estimate the extended state of the target.

How to partition the measurement set accurately and effectively is one of the main tasks of extended target tracking. In multiple extended target tracking, a single target generates multiple measurements, and with the interference of clutter, it is difficult to establish the correspondence between the measurements and the target. The ET-GM-PHD filtering algorithm needs to consider all partitions of the target measurement set, which is computationally difficult in practical applications. In application scenarios with a large number of targets and measurements, the DP algorithm has high computational complexity. In addition, it is essentially a hierarchical single-chain clustering algorithm, which lacks robustness and is sensitive to noise. In addition to DP, K-means++ clustering [15], spectral clustering [16], and expectation maximization (EM) [6] partitioning algorithms are also included. It is difficult to deal with measurement set partition in complex scenes using single partition method. Therefore, finding a combination of multiple clustering algorithms can bring more accurate division results and provide a guarantee for subsequent high-precision filtering. A comparison of the characteristics of existing extended object tracking algorithms based on different partitioning methods is presented in Table 1. In addition, in recent years, Ref. [17] proposed an algorithm to create data particles in two-dimensional feature space through its geometric partition (GD). This method solves the classification problem of datasets with similar centers of gravity and overlapping objects described by different labels. Therefore, the data particle geometric partition method has broad prospects for the measurement partition problem of multiple close distance targets. However, the drawback of this method is that it can only be applied to 2D datasets.

The number of measurements in the measurement set is the main factor that affects the speed and number of partitions. How to effectively reduce the number of measurements participating in clustering without affecting the accuracy of partitioning is the focus of this paper. To solve this problem, this paper proposes an extended multi-target tracking algorithm based on temporal correlation, which is based on ET-GM-PHD and GM-PHD filtering algorithms. The measurement set is hierarchically processed at the same time, which improves the filtering accuracy and reduces the computational complexity. Experimental results show that the proposed method improves the overall filtering performance compared with the DP partition algorithm.

To summarize, the main contributions of this work are listed as follows.

- A hierarchical measurement partitioning method based on spatio-temporal correlation is proposed;
- The ET-GM-PHD filter based on spatio-temporal correlation is proposed, and the corresponding implementation scheme is given;
- The performance of the proposed method is assessed via simulations.

The rest of this paper is organized as follows. Section 2 introduces relevant mathematical modeling. In Section 3, the ET-GM-PHD filter based on the spatio-temporal correlation

method is proposed. The simulation results of the proposed method are analyzed in Section 4. Conclusions are presented in Section 5.

Table 1. Extended target tracking algorithm based on different measurement partition methods.

Measurement Partition Method	Main Characteristic
Traditional method	Updating requires iterating over all possible subsets of measurement partitions
Algorithm based on distance partition [6,14]	The computational complexity is high, and it is difficult to accurately divide the measurement sub-set corresponding to the target in the case of a large number of targets and lacks robustness.
K-means++ clustering [15]	The center point needs to be found iteratively. When the number of targets is large and the distance is close, it is difficult to distinguish the measurement sets of different targets.
Spectral clustering [16]	This method is based on adjacency matrix propagation, which can divide the measurement set more accurately. However, this method is very sensitive to clutter, and it needs to eliminate the clutter in addition, and it is complex to deal with dense clutter scenes.
Expectation maximization (EM) [6]	The EM measurement partitioning algorithm converges to the nearest local maximum of the likelihood function. Since the EM partitioning is initialized using the predicted GIW components, the partitioning performance is sensitive to the maneuverability of the motion model and prediction results.
Spatio-temporal correlation (proposed)	The measurement set partitions are hierarchically processed simultaneously. The computational efficiency and accuracy are higher.

2. Mathematical Modeling

Multiple extended target tracking is used to estimate the number and motion state of multiple extended targets based on sensor observation data in a noisy environment. The number of targets and measurements changes over time with the birth, derivation, and death of targets and missed detection of sensors. Mahler proposed a multi-extended target tracking framework based on a Poisson multi-target model. In the RFS multi-extended filtering framework, the state and measurement of the target are, respectively, expressed as $X_k = \{x_k^1, \dots, x_k^{N_{x,k}}\} \in X$ and $Z_k = \{z_k^1, \dots, z_k^{N_{z,k}}\} \in Z$, where $x_k^{N_{x,k}}$ is the state of a single target and $N_{x,k}$ is the number of targets at time k . $z_k^{N_{z,k}}$ is a single measurement value and $N_{z,k}$ is the number of measurements at time k .

Since the prediction formula of ET-GM-PHD is the same as that of the standard GM-PHD filter, only the update formula of the ET-GM-PHD filter is considered here. The measurement update equation can be expressed as follows:

$$D_{k|k}(x|Z) = L_{Z_k}(x)D_{k|k-1}(x|Z) \tag{1}$$

where $L_{Z_k}(x)$ represents the measurement pseudo-likelihood function and is defined as follows:

$$L_{Z_k}(x) \triangleq 1 - \left(1 - e^{-\gamma(x)}\right)p_D(x) + e^{-\gamma(x)}p_D(x) \times \sum_{P \subset Z_k} \omega_P \sum_{W \in P} \frac{\gamma(x)^{|W|}}{d_W} \cdot \prod_{z_k \in W} \frac{\phi_{z_k}(x)}{\lambda_k c_k(z_k)} \tag{2}$$

where $P \subset Z_k$ denotes that the measurement set Z_k is divided into non-empty measurement units W ; $\phi_{z_k}(x) = p(z_k|x)$ represents the measurement likelihood function generated by a single target; $\gamma(x)$ represents the expected number of target measurements; $p_D(x)$ represents the probability of object detection; λ_k denotes the average number of clutter

measurements; and $c_k(z_k)$ is the uniform clutter density in the surveillance area. For more details of the ET-GM-PHD algorithm, we can refer to reference [14].

It can be seen from Equation (2) that, in the multi-extended target tracking framework, the measurement set needs to be divided, and the accuracy of the division result directly affects the subsequent filtering result. The DP algorithm proposed in reference [14] is a widely used measurement set partitioning method. This method uses the distance between the measurements to cluster, but when two or more extended targets are close to each other, the measurements belonging to different targets will fall into the same cluster unit after partitioning, resulting in the reduction in the number of measurement units. However, the number of measurement values in the existing measurement units increases. To solve this problem, Granstrom proposed a second partition method [14], which divided the divided measurement set again, but this method had a large amount of calculation and poor real-time tracking. In 2020, a research paper [18] used the method based on shared nearest neighbors (SNN) of directed graph to divide the measurement values. These two methods do not consider the correlation between adjacent extended target measurements. Therefore, this paper proposes a partition method of an extended target measurement set, based on spatio-temporal correlation.

3. Partition Method Based on Spatio-Temporal Correlation

Considering the correlation between the adjacent measurements and the target motion model, this paper proposes a fast partition and hierarchical processing algorithm for the measurement set. When multiple extended targets cross or are close to each other, the algorithm can also achieve accurate cardinality estimation and target state estimation, and greatly reduces the amount of calculation. At the same time, the method is not affected by the measurement density.

The partitioning method proposed in this paper mainly includes two parts: partitioning the living target measurement set and partitioning the newborn target measurement set. Firstly, the two basic clustering algorithms used in this method are K-means++ clustering algorithm and DBSCAN clustering algorithm.

3.1.1. The K-Means++ Clustering Algorithm

In multiple extended target tracking, since the measurement set at each time contains measurements from different targets and clutter, it is necessary to use a clustering algorithm to cluster the measurement set, i.e., measurement set partition. The K-means clustering algorithm is a kind of commonly used clustering algorithm, wherein K denotes the number of clusters. Since the number of extended targets and clutter varies at different times, K is also time-varying. If the K traversal interval is $[K_L, K_U]$ (where $K_L = 1, K_U = |Z_k|$), the number of measurement partitions will be quite large when the number of measurements is large, so the value range needs to be narrowed. In addition, the K-means clustering algorithm is unstable because it randomly selects the initial points.

To solve the above problems, the K-means++ algorithm was proposed in the literature [15]. The specific algorithm steps are as follows:

1. Randomly select a center from the dataset c_1 ;
2. Select the next central point c_i with probability $\frac{D(x')}{\sum_{x \in X} D(x)^2}$, $x' \in X$;
3. Repeat step 2 until there are k central points, $\mathcal{C} = \{c_1, c_2, \dots, c_k\}$;
4. For each $i \in \{1, \dots, k\}$, set the cluster C_i to be the point set in X that is closer to c_i than c_j , where $i \neq j$;
5. For each $i \in \{1, \dots, k\}$, let c_i be the centroid of all points in C_i , $c_i = \frac{1}{|C_i|} \sum_{x \in C_i} x$;
6. Repeat steps 4 to 5 until \mathcal{C} is no changes.

3.1.2. The DBSCAN Clustering Algorithm

DBSCAN is a density-based clustering algorithm. The algorithm divides the entire sample set quickly by using the sample sets which are closely connected in each group. Simultaneously, the algorithm groups closely connected sample sets into one class to form a cluster category, while not requiring the prior input of the number of samples for clustering. The basic idea of DBSCAN clustering algorithm is that, for each measurement in the partition cell, the neighborhood of its given radius contains no less than a given number of measurements.

Therefore, DBSCAN only needs two input parameters: the size of the radius and the minimum number of measurements in the neighborhood of each measurement in the partition cell. For a sample set of any shape, there exists some point from which any point in the sample set can be reached by a “dense” path. In other words, the points in the cluster must be density-connected.

Suppose that, at time k , it exists a set of measurements $Z = \{z^i\}_{i=1}^{N_z}$ (subscript k is ignored for simplicity). If a measurement is a core point, then its neighborhood ε (see reference [19] for a definition of neighborhood) contains at least M measurements.

The steps of the DBSCAN algorithm are described as follows:

1. Set the cluster count $\mathcal{C} = 0$ and the set of core points $C = \{\}$;
2. Traverse the measurement z^i values in the measurement set Z , and determine whether it is a core point. If it is, add it to the set C , i.e., $C = C \cup \{z^i\}$;
3. Traverse the set of core points z^i in C that have not been visited. Increment the cluster count $\mathcal{C} = \mathcal{C} + 1$. Set the category of z^i as \mathcal{C} and marked it as visited.
4. According to the current core point z^i and the count of clusters \mathcal{C} , traverse all points z^j in the ε neighborhood of z^i , setting the category of z^j as \mathcal{C} and marking them as visited. If z^j is not visited and is a core point, set $z^i = z^j$ and repeat step 4 until the condition is not satisfied;
5. Repeat steps 3 and 4 until all the core points are visited;
6. The points in the measurement set Z that do not belong to the core points and have not been visited are set as noise points.

After the above steps, the measurement set Z is divided into the measurement set of the target and the noise point.

3.2. Division of Survival Target Measurement Set

For an extended target that survives at time k , according to its motion model, the target position at the previous time is correlated with the target position at the current time, and the measurements generated by the extended target at these two times are also correlated. The measurement set at time k is set to $Z_k = \{z_k^{(i)}\}_{i=1}^{n_k}$, n_k denotes the number of measurements at time k , and the prediction of the Gaussian term of the ET-GM-PHD filter is $\{w_{k|k-1}^i, m_{k|k-1}^i, P_{k|k-1}^i\}_{i=1}^{J_{k|k-1}}$, where $J_{k|k-1}$ is the number of Gaussian components. The process of dividing the living target measurement set is described as follows:

1. Select the measurement set of the surviving targets. The components with weights larger than 0.5 in the Gaussian term of time prediction are selected, which is denoted by $G_s = \{\hat{w}_k^i, \hat{m}_k^i, \hat{P}_k^i\}_{i=1}^{J_{k,s}}$, and their position components are extracted as the centroid estimation of the surviving target, which is denoted by $x_k^i, i = 1, \dots, J_{k,s}$. Then the candidate measurement set of the i th extended target at time k is given by the following:

$$\tilde{Z}_k^i = \{z_k^j | z_k^j \in Z_k, d(z_k^j, x_k^i) < \varepsilon\} \tag{3}$$

2. Determine the class of the cluster. If $\tilde{Z}_k^i = \emptyset$, it means that the i th extended target at time k has died, the number of surviving extended targets is decreased by one, and the number of surviving targets at time k is finally determined as c_k .

- Cluster the living target measurements. For the set of measurements obtained in step 1, its union is \tilde{Z}_k . This dataset is put into the K-means++ clustering algorithm, and the i th cluster center is obtained as $\hat{x}_k^i, i = 1, \dots, c_k$, which can be regarded as the centroid estimation of the i th extended target. At this point, the tracking of the extended target is converted to the tracking of the point targets, and the estimated value of the centroid is brought into the update formula of GM-PHD, and the updated Gaussian term is $\{w_k^i, m_k^i, P_k^i\}_{i=1}^{c_k}$.

3.3. Division of Newborn Target Measurement Set

It is assumed that the location of the newborn target and the living target are far apart in the sensor monitoring area, so that the measurements of the living target and the newborn target are less correlated. Under this assumption, the measurements of the newborn target do not exist in the set \tilde{Z}_k , so $Z_L = Z_k - \tilde{Z}_k$ will only include the measurements of the newborn target (if there is a newborn target at the current time) and clutter measurements.

The steps of measurement set division for newborn targets are as follows:

- The measurement set Z_L is brought into the processing step of the DBSCAN clustering algorithm for preprocessing. The purpose of this step is to remove the clutter, where $M = 4$ is the minimum number of measurements contained in the neighborhood ϵ ($\epsilon = 100$) of the measurement. Furthermore, determine whether there is a cluster unit in the set; if so, go to step 2; otherwise, go to step 4.
- The set of measurements processed by the DBSCAN clustering algorithm is \tilde{Z}_k , the number of clusters is $K_p > 0$, and \tilde{Z}_k only consists of measurements generated by extended targets. To this end, a novel SNN method based on directed k-nearest neighbors (kNN) graph is used to cluster, for $\tilde{Z}_k = \{z_k^i\}_{i=1}^n, k = 8$. The SNN of a directed kNN graph is defined as follows:

$$N_i \cap N_j = \begin{cases} N_i \cap N_j \cup \{z^{ij}\} & \text{if } z^i \leftrightarrow z^j \\ N_i \cap N_j & \text{otherwise} \end{cases} \quad (4)$$

Following the above definition, the similarity between two centers of mass in a directed kNN graph is calculated as follows:

$$w_{ij} = \sum_{z^s \in N_i \cap N_j} (k - i_s^{th} + 1)(k - j_s^{th} + 1) \quad (5)$$

The specific method is described as follows:

- Calculate the similarity matrix W of the measurement set \tilde{Z}_k according to the similarity defined in Equation (5), i.e.,

$$W = \begin{pmatrix} w_{11} & w_{12} & \dots & w_{1n} \\ w_{21} & w_{22} & \dots & w_{2n} \\ \vdots & \vdots & \dots & \vdots \\ w_{n1} & w_{n2} & \dots & w_{nn} \end{pmatrix} \quad (6)$$

Then, the dimension of W is $n \times n$, and W is an asymmetric matrix.

- Spectral clustering is used to solve the graph partition problem for the calculated similarity matrix W . First, we compute the unnormalized Laplacian matrix L , as follows:

$$L = D - W \quad (7)$$

where

$$D = \begin{pmatrix} d_1 & 0 & \cdots & 0 \\ 0 & d_2 & \cdots & 0 \\ \vdots & \vdots & \ddots & \vdots \\ 0 & 0 & \cdots & d_n \end{pmatrix} = \begin{pmatrix} \sum_{j=1}^n w_{1j} & 0 & \cdots & 0 \\ 0 & \sum_{j=1}^n w_{2j} & \cdots & 0 \\ \vdots & \vdots & \ddots & \vdots \\ 0 & 0 & \cdots & \sum_{j=1}^n w_{nj} \end{pmatrix} \quad (8)$$

- Calculate the normalized Laplacian matrix $L^s = D^{-1/2}LD^{-1/2}$.
- Build the matrix U . Since the matrix U is not a binary representation, we treat it as a new data matrix, which is denoted by the following:

$$U = \begin{pmatrix} | & | & \cdots & | \\ u_n & u_{n-1} & \cdots & u_{n-K+1} \\ | & | & \cdots & | \end{pmatrix} = \begin{pmatrix} u_{n,1} & u_{n-1,1} & \cdots & u_{n-K+1,1} \\ u_{n,2} & u_{n-1,2} & \cdots & u_{n-K+1,2} \\ \vdots & \vdots & \ddots & \vdots \\ u_{n,n} & u_{n-1,n} & \cdots & u_{n-K+1,n} \end{pmatrix} \quad (9)$$

where K denotes the number of clusters, $K \in [K_l, K_u]$, $K = K + 1$, $K_l = K_p$, $K_u = K_l + \lceil \frac{n}{\beta} \rceil$, n is the number of measurements in the measurement set \tilde{Z}_k , and β is the measurement rate of the extended target.

- Normalize each row of the matrix U as follows:

$$y_i = \frac{1}{\sqrt{\sum_{j=1}^K u_{n-j+1,i}^2}} (u_{n,i}, u_{n-1,i}, \dots, u_{n-K+1,i})^T \quad (10)$$

$Y = \{y_1^T, \dots, y_n^T\} \in \mathbb{R}^{n \times K}$ is obtained. Each row in the matrix Y is clustered as a new data point in the K dimensional space, and the K-means++ clustering algorithm is used to obtain the clustering results $C = \{C_1, \dots, C_K\}$. The measurement z_k^i belongs to the j th class, when the i th row of the matrix Y is clustered into the j th class. The set of measurements \tilde{Z}_k is then partitioned into K classes, and $K \in [K_l, K_u]$, $K = K + 1$. Then, a clustering result $class(K)$ of the measurement set \tilde{Z}_k is obtained.

- Repeat the previous step until the condition $K \in [K_l, K_u]$ is not satisfied, and finally obtain the measurement division result $P_k = \bigcup_{K \in [K_l, K_u]} class(K)$ at time k .
3. For each partition result $class(K)$, the Gaussian term $\{w_{k|k-1}^i, m_{k|k-1}^i, P_{k|k-1}^i\}_{i=1}^{J_{k|k-1}} \cup \{w_{k,B}^i, m_{k,B}^i, P_{k,B}^i\}_{i=1}^{n_B}$ is updated in the update step of ET-GM-PHD filtering algorithm, and the updated Gaussian term is given by $\{w_k^i, m_k^i, P_k^i\}_{i=1}^{J_u}$.
 4. The union of the updated Gaussian terms is $\{w_k^i, m_k^i, P_k^i\}_{i=1}^{J_c+J_u}$. After pruning and merging, the target state at time k is extracted.

The proposed algorithm is shown in Figure 1. Firstly, the measurement set is divided into the living target measurement set and the newborn target measurement set, and the computational complexity is $O(|Z|)$. For the surviving target measurement set, since the number of clusters required is known in advance, the computational complexity of K-means++ is $O(n_k^2)$, where n_k is the number of surviving targets, and the computational complexity of GM-PHD update step is $O(J_{k-1} \times n_k)$, where J_{k-1} is the number of Gaussian components at the previous time. For the newly born target measurement set, the computational complexity is, at most, $O(|Z_L|^2)$. Suppose that the number of remaining

measurements in the measurement set Z_L after processing by DBSCAN algorithm is N , the computational complexity of spectral clustering is, at most, $O(N^3)$. When the number of measurements is large, the k of the directed kNN graph is far less than N , and its similarity matrix is the sparse matrix, so the calculation efficiency is high. Assume that the number of edges of the directed kNN graph is m and the computational complexity of the eigenvector is $O(m \times N)$. The computational complexity of the ET-GM-PHD update step is $O\left(J_{k-1} + n_x^2 \sum_p^P P_p\right)$, where P_p denotes the number of partitions and n_x is the number of iterations, while the time complexity of distance partition is $O(|Z|^4)$.

Remark 1. When there are a large number of extended targets in the scene, and the extended targets are close to each other and move in parallel with variable speed, the distance division method only may fail to divide the measurement set. In order to improve the tracking performance, on the basis of the method proposed in this paper, multiple methods can be combined to further accurately divide the target measurement set, including gating, partitioning, assignment, etc. [6,20–22].

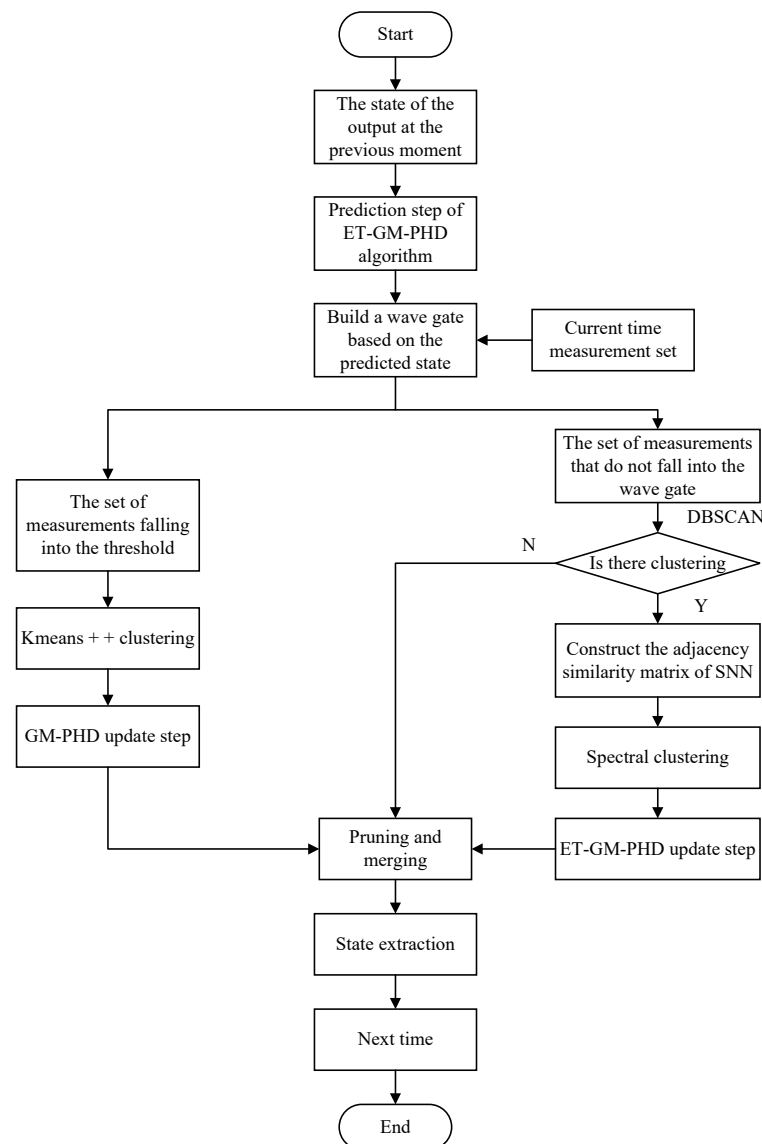


Figure 1. Partitioning method based on spatio-temporal correlation.

The flowchart of the computational complexity involved in each block of the proposed tracking method is presented in Figure 2.

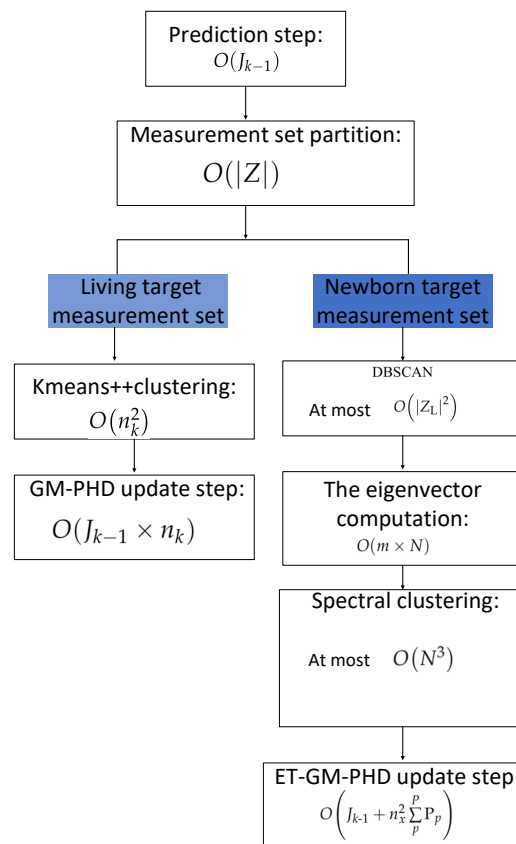


Figure 2. The flowchart of the computational complexity involved in each block.

4. Simulation Results and Analysis

In order to verify the effectiveness of the proposed algorithm in this paper, this paper implements the ET-GM-PHD filtering algorithm, based on the algorithm proposed in this paper, distance partition [14] and directed graph SNN partition [18]. The simulation platform is MATLAB, R2018b, Win10 64-bit professional operating system, i7-9700@3.00 GHz, 16.00 GB RAM.

The bird’s eye view of the multi-object tracking scenario considered in this paper is shown in Figure 3.

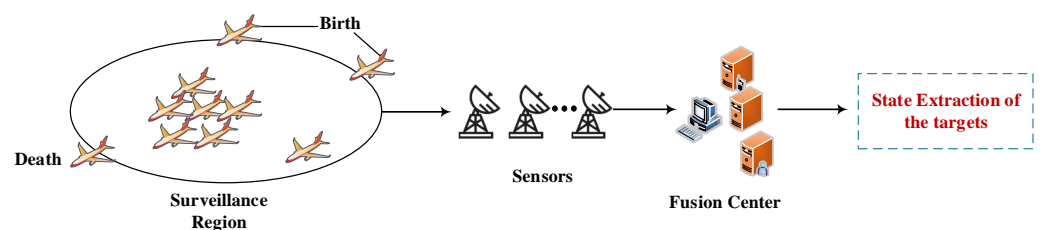


Figure 3. The bird’s eye view of the multi-object tracking scenario.

The evaluation method of OSPA [23] is adopted to calculate the OSPA error of the filtering algorithm based on different division methods. In this simulation experiment, OSPA parameters are set as $p = 2$ and $c = 60$, respectively. The number of Monte Carlo simulation experiments is 100. For fair comparison, the subsequent simulation experiments are the same as the simulation scenarios in the literature [18]. In the simulation, the target

kinematic model adopts the CV (constant velocity) model, and the state transition matrix is given by the following:

$$F = \begin{bmatrix} 1 & T_s & 0 & 0 \\ 0 & 1 & T_s & 0 \\ 0 & 0 & 1 & 0 \\ 0 & 0 & 0 & 1 \end{bmatrix} \quad (11)$$

where the sampling interval $T_s = 1$ s in this simulation.

The process noise covariance matrix is $Q = \sigma_v^2 \begin{bmatrix} \frac{T_s^4}{4} I_2 & \frac{T_s^3}{2} I_2 \\ \frac{T_s^3}{2} I_2 & \frac{T_s^2}{4} I_2 \end{bmatrix}$, the measurement noise covariance matrix is $R = \sigma_\epsilon^2 I_2$, where I_2 is a 2×2 identity matrix, the process noise standard deviation is set as $\sigma_v = 2$, and the measurement noise standard deviation is set as $\sigma_\epsilon = 20$.

The size of the area monitored by the sensor is $[-1000, 1000]$ m \times $[-1000, 1000]$ m. To verify the performance of the algorithm, the survival probability of each target is set as $P_s = 0.95$, with the detection probability of $P_d = 0.95$. The number of extended target measurements is a Poisson distribution with an expectation value of 10. The clutter measurements are uniformly distributed in the detection area, while the clutter count follows a Poisson distribution with an expected value of 20.

To ensure the feasibility of the algorithm, the Gaussian terms need to be pruned and merged. The maximum number of Gaussian components is $J_{\max} = 100$, with the pruning threshold $T = 10^{-6}$, the merging threshold $U = 4$, and the distance threshold $\sigma = 50$.

4.1. Simulation Experiment 1

To verify the effectiveness of the proposed algorithm, two extended target cross motion scenes are constructed. The survival time of both extended target 1 and extended target 2 is 1~100 s, and there are no derived targets in the scenario. The intensity function of the newborn target is given by the following:

$$\gamma_t(x) = 0.1\mathcal{N}(x; m_{\gamma,t}^{(1)}, P_{\gamma,t}) + 0.1\mathcal{N}(x; m_{\gamma,t}^{(2)}, P_{\gamma,t}) \quad (12)$$

where $m_{\gamma,t}^{(1)} = [250 \text{ m}, 250 \text{ m}, 0 \text{ m/s}, 0 \text{ m/s}]^T$, $m_{\gamma,t}^{(2)} = [-250 \text{ m}, -205 \text{ m}, 0 \text{ m/s}, 0 \text{ m/s}]^T$, $P_{\gamma,t} = \text{diag}([100, 100, 25, 25])$. The real tracks of the targets in the scene are shown in Figure 4a, which shows that the tracks of the two extended targets cross at 56 s. Figure 4b shows the running results of the proposed algorithm under a single simulation. It can be seen from the figure that the state estimation of the target is also accurate when the extended target tracks cross.

Figure 5a shows the OSPA distance comparison of different algorithms under 100 Monte Carlo simulations. It can be seen from the figure that the proposed algorithm OSPA distance is the minimum, even at the extended target track crossing moment. The OSPA distance gap between the algorithm, based on the directed graph partitioning of SNN, and the distance partitioning method is very small. Specifically, the OSPA distance of the directed SNN graph partition is significantly smaller in several adjacent moments when the targets cross. The comparison plot of OSPA distance verifies the effectiveness of the proposed algorithm.

Figure 5b gives a comparison plot of the extended target number estimation. It can be seen from the figure that, since the two targets intersect at 56 s, the extended target at the current moment is close to the extended target at several adjacent moments. Thus, when the measurement set is partitioned by distance partition and directed graph SNN partition methods, measurements of different extended targets fall into the same set, resulting in the potential estimation error, and the potential error of graph partition method is smaller. The method proposed in this paper takes into account the correlation of the extended targets at adjacent times, so that it can achieve accurate potential estimation when the targets are close to each other or cross.

Figure 6a,b shows the average number of partitions and the average running time of the measurement set at each time, respectively. It can be seen from the figures that distance partition has the highest average number of splits and the highest running time, because the distance partition needs to traverse multiple distance thresholds to find the best set of measurement partitions. The number of partitions of the directed graph SNN ranks second, and it first uses the DBSCAN algorithm to filter out part of the clutter, so the number of set partitions is smaller. The average number of partitions proposed in this paper is the lowest, which basically requires only one partition of the measurement set. When the extended target tracks cross, the measurement distance is close, and the number of distance division will be reduced at this time. At the same time, the running time of the algorithm reflects the number of partitions.

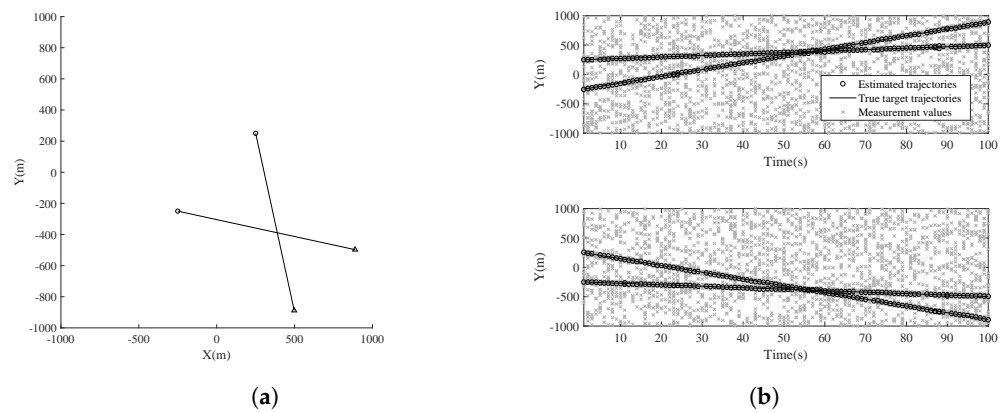


Figure 4. (a) Real trajectory of the targets in Scenario 1. (b) Measurement values, true target trajectories, and estimated trajectories in Scenario 1.

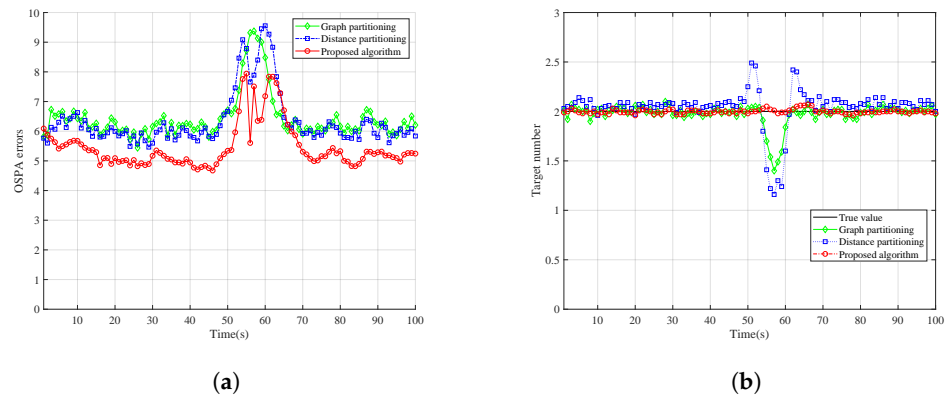


Figure 5. (a) Measurement values, true target trajectories, and estimated trajectories in Scenario 1. (b) Comparison of OSPA errors under Scenario 1.

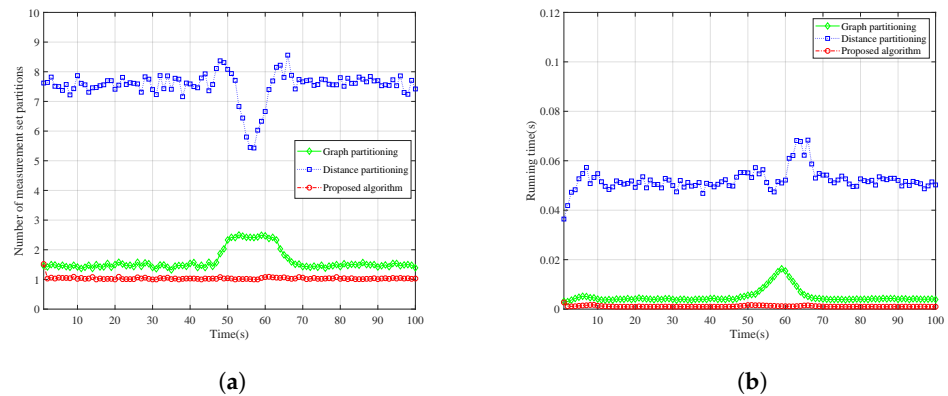


Figure 6. (a) Comparison of the number of measurement set partitions in Scenario 1. (b) Comparison of running time of each algorithm for Scenario 1.

4.2. Simulation Experiment 2

The purpose of this experiment is to verify the filtering performance of the proposed algorithm for targets in scenarios where the extended targets are close to each other and moving in parallel. The survival time of extended target 1 and extended target 2 is both 1–100 s. The strength function of the newborn target in this scenario is given by the following:

$$\gamma_t(x) = 0.1\mathcal{N}(x; m_{\gamma,t}^{(1)}, P_{\gamma,t}) + 0.1\mathcal{N}(x; m_{\gamma,t}^{(2)}, P_{\gamma,t}) \quad (13)$$

where $m_{\gamma,t}^{(1)} = [-600 \text{ m}, -500 \text{ m}, 0 \text{ m/s}, 0 \text{ m/s}]^T$, $m_{\gamma,t}^{(2)} = [-600 \text{ m}, -600 \text{ m}, 0 \text{ m/s}, 0 \text{ m/s}]^T$.

The real target track of the target in scenario 2 is shown in Figure 7a, which consists of two parallel moving extended targets that are close to each other. Figure 7b shows the simulation results of the proposed algorithm. It can be seen from the figure that the kinematic state of the extended targets can be estimated relatively accurately even when the distance between the extended targets is close.

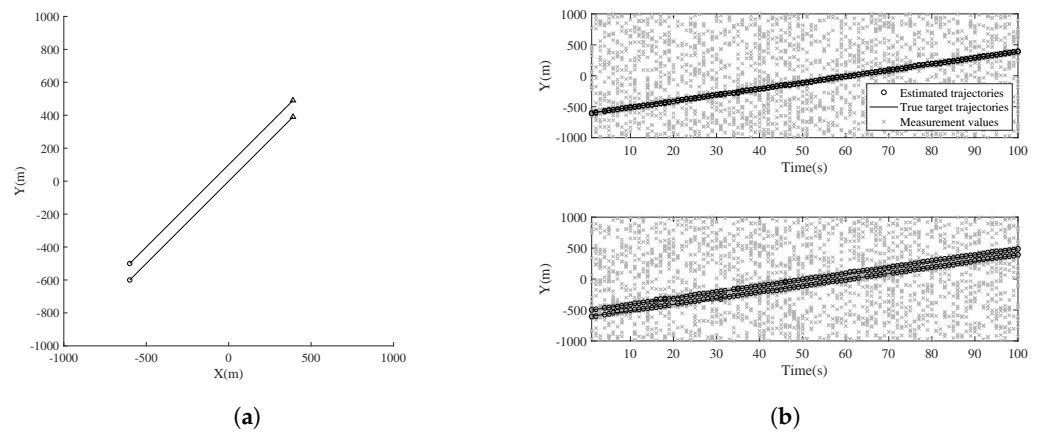


Figure 7. (a) Real trajectory plot of the target in Scenario 2. (b) Measurement values, true target trajectories, and estimated trajectories in Scenario 2.

Figure 8a shows the OSPA distance comparison diagram of the three partitioning methods for scenario 2, and the OSPA distance index is calculated by the comprehensive calculation of the extended target state estimation and the target number estimation. It can be seen from the figure that the proposed algorithm has the smallest OSPA distance and the most accurate target number estimation at the same time. Scenes of parallel moving objects that are close to each other also verify the effectiveness of the algorithm. Meanwhile, the comparison figure of the target number estimation in Figure 8b also reflects the effectiveness of the algorithm, and the target number estimation of the proposed algorithm is significantly better than that of the other two algorithms.

Figure 9a,b shows the average number of partitions and the average running time of the measurement set partition at each time, respectively. The figures show that the partition method proposed in this paper has the least number of partitions and the least running time. Since the proposed algorithm considers the relevance of the adjacent time of the extended target, the measurement set of the surviving target is divided by using the prior information, which greatly reduces the number of undivided measurements in the measurement set and the number of partitions.

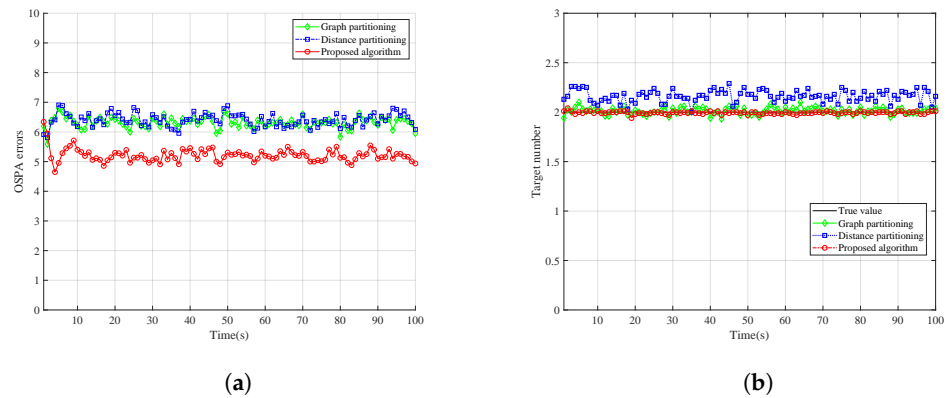


Figure 8. (a) Comparison of OSPA errors for Scenario 2. (b) Comparison of target number estimation in Scenario 2.

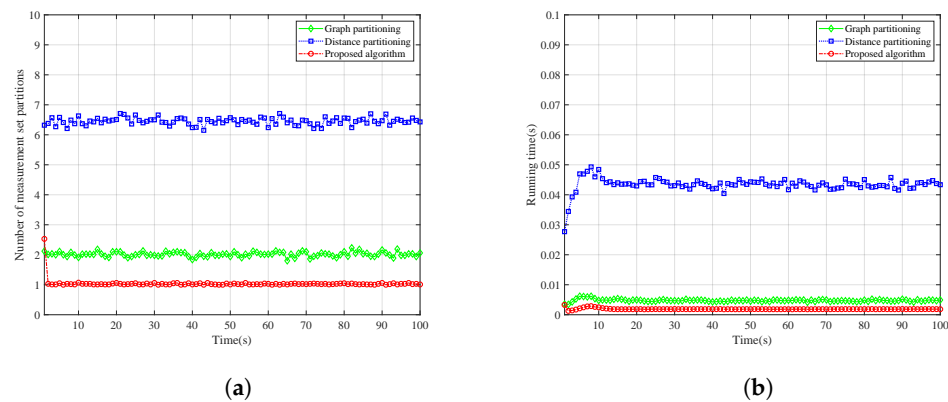


Figure 9. (a) Comparison of measurement set partition number in Scenario 2. (b) Comparison of running times of each algorithms for Scenario 2.

4.3. Simulation Experiment 3

The goal of this experiment is to verify the effectiveness of the proposed algorithm for the birth and death scenarios of multiple extended targets. The strength function of the newborn target is given by the following:

$$\begin{aligned} \gamma_t(x) = & 0.1\mathcal{N}(x; m_{\gamma,t}^{(1)}, P_{\gamma,t}) + 0.1\mathcal{N}(x; m_{\gamma,t}^{(2)}, P_{\gamma,t}) \\ & + 0.1\mathcal{N}(x; m_{\gamma,t}^{(3)}, P_{\gamma,t}) + 0.1\mathcal{N}(x; m_{\gamma,t}^{(4)}, P_{\gamma,t}) \end{aligned} \quad (14)$$

where $m_{\gamma,t}^{(1)} = [100 \text{ m}, 450 \text{ m}, 0 \text{ m/s}, 0 \text{ m/s}]^T$, $m_{\gamma,t}^{(2)} = [-450 \text{ m}, -450 \text{ m}, 0 \text{ m/s}, 0 \text{ m/s}]^T$, $m_{\gamma,t}^{(3)} = [450 \text{ m}, -209 \text{ m}, 0 \text{ m/s}, 0 \text{ m/s}]^T$, $m_{\gamma,t}^{(4)} = [-350 \text{ m}, -350 \text{ m}, 0 \text{ m/s}, 0 \text{ m/s}]^T$. Figure 10a shows the real tracks of multiple extended targets in Scenario 3. Figure 10b shows the simulation results of the proposed algorithm.

Figure 11a shows the OSPA distance comparison of the three partition methods in scenario 3. It can be seen from the figure that the proposed method has the smallest OSPA distance. However, at the 27th and 76th seconds, the OSPA distance becomes larger, which is because there are newborn targets appearing at these two moments. Figure 11b shows the comparison of target number estimation. As can be seen from the figure, the cardinality estimation of the proposed algorithm is significantly better than the other two algorithms when the number of targets in the scene is large.

Figure 12a,b show the average number of partitions and the average running time of the three methods. The proposed method has the lowest number of partitions and running time. Since the proposed method not only makes full use of the prior information, but

also converts point target tracking into extended target tracking, the number of distance partitions increases with the number of objects in the scene.

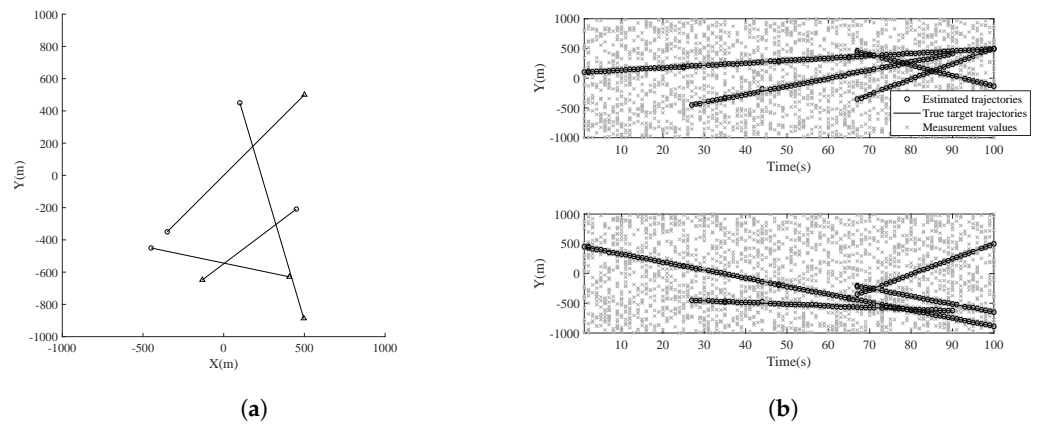


Figure 10. (a) Real target trajectory for Scenario 3. (b) Measurement values, true target trajectories, and estimated trajectories in Scenario 3.

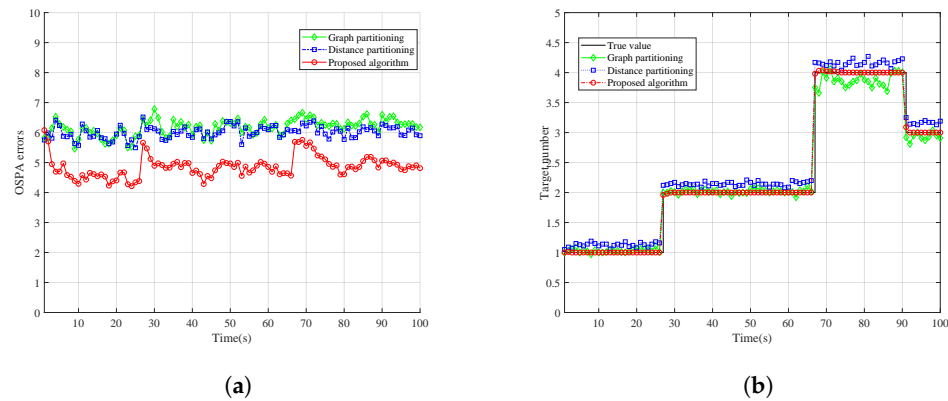


Figure 11. (a) Comparison of OSPA errors for Scenario 3 (b) Comparison of target number estimation in Scenario 3.

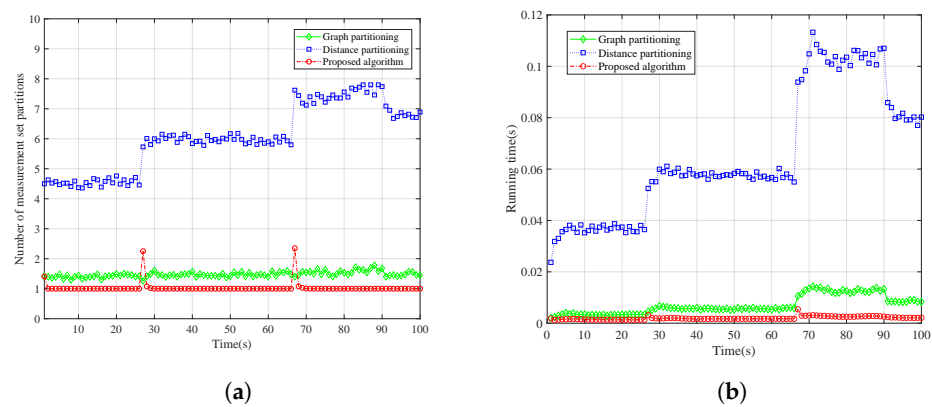


Figure 12. (a) Comparison of measurement set partition number in Scenario 3. (b) Comparison of running times of each algorithms for Scenario 3.

4.4. Simulation Experiment 4

The purpose of this experiment is to verify the filtering performance of the proposed algorithm in the variable velocity case in case of variable velocity. We consider adding a constant turn (CT) model, i.e.,

$$F = \begin{bmatrix} 1 & \sin(T_s\omega)/\omega & 0 & -(1 - \cos(T_s\omega))/\omega \\ 0 & \cos(T_s\omega) & 0 & -\sin(T_s\omega) \\ 0 & (1 - \cos(T_s\omega))/\omega & 1 & \sin(T_s\omega)/\omega \\ 0 & \sin(T_s\omega) & 0 & \cos(T_s\omega) \end{bmatrix} \tag{15}$$

$$Q_{CT} = q_{\tau_2} \begin{bmatrix} T_s^4/4 & T_s^3/2 & 0 & 0 \\ T_s^3/2 & T_s^2 & 0 & 0 \\ 0 & 0 & T_s^4/4 & T_s^3/2 \\ 0 & 0 & T_s^3/2 & T_s^2 \end{bmatrix} \tag{16}$$

where $q_{\tau_2} = 0.0016$, ω denotes the rotational angular velocity, and T_s denotes the sampling period.

The strength function of the newborn target is given by the following:

$$\gamma_t(x) = 0.1\mathcal{N}(x; m_{\gamma,t}^{(1)}, P_{\gamma,t}) + 0.1\mathcal{N}(x; m_{\gamma,t}^{(2)}, P_{\gamma,t}) + 0.1\mathcal{N}(x; m_{\gamma,t}^{(3)}, P_{\gamma,t}) \tag{17}$$

where

$$m_{\gamma,t}^{(1)} = [-1300 \text{ m}, 5 \text{ m/s}, 500 \text{ m}, -5 \text{ m/s}]^\top \tag{18}$$

$$m_{\gamma,t}^{(2)} = [50 \text{ m}, 8 \text{ m/s}, 50 \text{ m}, 8 \text{ m/s}]^\top \tag{19}$$

$$m_{\gamma,t}^{(3)} = [-550 \text{ m}, -6 \text{ m/s}, -650 \text{ m}, 6 \text{ m/s}]^\top \tag{20}$$

The motion model for Scenario 4 is shown in Table 2.

Table 2. Trajectory configurations in Scenario 4.

Target	Dynamic Models	Model Duration Time	Birth Time	Death Time
1	CV	1–10 s, 60–70 s, 87–100 s	1 s	100 s
	CT	11–59 s, 71–86 s		
2	CV	1–10 s, 60–70 s, 87–100 s	1 s	100 s
	CT	11–59 s, 71–86 s		
3	CV	1–10 s, 60–70 s, 87–100 s	1 s	100 s
	CT	11–59 s, 71–86 s		

Figure 13a shows the real tracks of multiple extended targets in Scenario 4. Figure 13b shows the OSPA distance comparison of the three partition methods in scenario 4. It can be seen from the figure that the proposed method has the smallest OSPA distance. However, at the 1st–5th seconds, the OSPA distance becomes larger, which is because there are newborn targets. Figure 14a,b shows the average number of partitions and the average running time of the three methods. The proposed method has the lowest number of partitions and running time. The reason is that the proposed method not only makes full use of the prior information, but also converts point target tracking into extended target tracking. Figure 14c shows the comparison of target number estimation. As can be seen from the figure, the cardinality estimation of the proposed algorithm is significantly better than the other two algorithms.

From the simulation results, we can see that the performance of the proposed algorithm is still better than the other two comparison methods in the variable velocity scenario with a CT model.

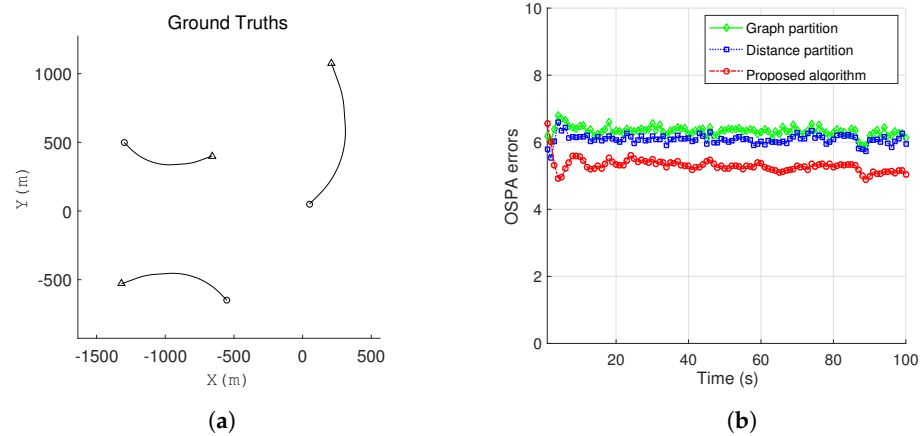


Figure 13. (a) Real target trajectory for Scenario 4. (b) Comparison of OSPA errors in Scenario 4.

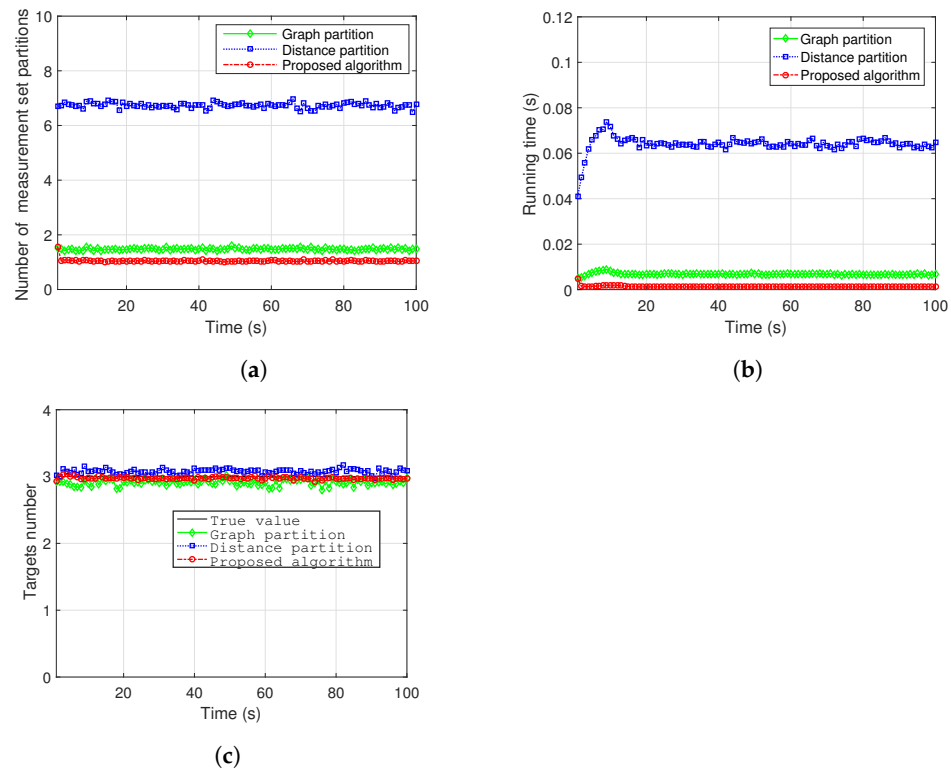


Figure 14. (a) Comparison of measurement set partition number in Scenario 4. (b) Comparison of running times of each algorithms for Scenario 4. (c) Comparison of target number estimation in Scenario 4.

5. Conclusions

This paper focuses on the measurement set partition problem for extended target tracking in a clutter environment. Based on the idea of spatio-temporal correlation, the ET-GM-PHD filter based on the directed graph SNN is proposed, and the corresponding implementation scheme is given. Simulation results show that the method is effective. In addition, in the process of target tracking, the tracking of the extended target is converted to the tracking of the point target, which effectively reduces the amount of calculation. In the future, we will verify the proposed algorithm in practical scenarios. In addition, to ensure the security of tracking results and prevent information interception, it is urgent to study how to use the estimated target results to identify the observation platform (estimation problem of stealth estimator) [24].

Author Contributions: Conceptualization, W.Z. and L.G.; methodology, W.Z. and C.L.; validation, W.Z., C.L. and T.L.; formal analysis, W.Z., C.L. and T.L.; investigation, L.G. and W.Z.; writing—original draft preparation, W.Z. and C.L.; writing—review and editing, T.L. and L.G.; supervision, L.G. All authors have read and agreed to the published version of the manuscript.

Funding: This research received no external funding.

Institutional Review Board Statement: Not applicable.

Informed Consent Statement: Not applicable.

Data Availability Statement: The original contributions presented in the study are included in the article, further inquiries can be directed to the corresponding author.

Conflicts of Interest: The funders had no role in the design of the study; in the collection, analyses, or interpretation of data; in the writing of the manuscript; or in the decision to publish the results.

Abbreviations

MTT	Multi-target tracking
ET	Extended target
RM	Random matrix
RHM	Random hypersurface model
GP	Gaussian process
RFS	Random finite set
MB	Multi-Bernoulli
DP	Distance partition
EM	Expectation maximization
PHD	Probability hypothesis density
GM	Gaussian mixture
GIW	Gaussian-inverse-Wishart
CV	Constant velocity
PMF	Probability mass function
EOs	Extended objects
OSPA	Optimal sub-pattern assignment
PDF	Probability density Function

References

1. Bar-Shalom, Y.; Kirubarajan, T.; Li, X.R. *Estimation with Applications to Tracking and Navigation*; John Wiley & Sons, Inc.: Hoboken, NJ, USA, 2001.
2. Waxman, M.J.; Drummond, O.E. A bibliography of cluster (group) tracking. *Proc. SPIE Int. Soc. Opt.* **2004**, *5428*, 551–560.
3. Granstrom, K.; Baum, M. Extended Object Tracking: Introduction, Overview and Applications. *J. Adv. Inf. Fusion* **2017**, *12*, 139–174.
4. Gilholm, K.; Salmond, D. Spatial distribution model for tracking extended objects. *IEE Proc. Radar Sonar Navig.* **2005**, *152*, 364–371. [[CrossRef](#)]
5. Koch, J.W. Bayesian Approach to Extended Object and Cluster Tracking using Random Matrices. *IEEE Trans. Aerosp. Electron. Syst.* **2008**, *44*, 1042–1059. [[CrossRef](#)]
6. Granstrom, K.; Orguner, U. A PHD Filter for Tracking Multiple Extended Targets Using Random Matrices. *IEEE Trans. Signal Process.* **2012**, *60*, 5657–5671. [[CrossRef](#)]
7. Baum, M.; Hanebeck, U.D. Shape tracking of extended objects and group targets with star-convex RHMs. In Proceedings of the 2011 14th Conference on Information Fusion, Chicago, IL, USA, 1–8 July 2011.
8. Özkan, E.; Wahlstrom, N. Extended Target Tracking Using Gaussian Processes. *IEEE Trans. Signal Process.* **2015**, *63*, 4165–4178.
9. Mahler, R.P.S.; Ebrary, I. *Statistical Multisource-Multitarget Information Fusion*; Artech House, Inc.: St. Norwood, MA, USA, 2007.
10. Vo, B.N.; Ma, W.K. The Gaussian Mixture Probability Hypothesis Density Filter. *IEEE Trans. Signal Process.* **2006**, *54*, 4091–4104. [[CrossRef](#)]
11. Vo, B.T.; Vo, B.N.; Cantoni, A. Analytic Implementations of the Cardinalized Probability Hypothesis Density Filter. *IEEE Trans. Signal Process.* **2007**, *55*, 3553–3567. [[CrossRef](#)]
12. Vo, B.T.; Vo, B.N.; Cantoni, A. The Cardinality Balanced Multi-Target Multi-Bernoulli Filter and Its Implementations. *IEEE Trans. Signal Process.* **2009**, *57*, 409–423.
13. Vo, B.N.; Vo, B.T.; Phung, D. Labeled Random Finite Sets and the Bayes Multi-Target Tracking Filter. *IEEE Trans. Signal Process.* **2014**, *62*, 6554–6567. [[CrossRef](#)]

14. Granstrom, K.; Lundquist, C.; Orguner, O. Extended Target Tracking using a Gaussian-Mixture PHD Filter. *IEEE Trans. Aerosp. Electron. Syst.* **2012**, *48*, 3268–3286. [[CrossRef](#)]
15. Arthur, D.; Vassilvitskii, S. K-Means++: The Advantages of Careful Seeding. In Proceedings of the Eighteenth Annual ACM-SIAM Symposium on Discrete Algorithms, SODA 2007, New Orleans, LO, USA, 7–9 January 2007.
16. Yang, J.; Liu, F.; Ge, H.; Yuan, Y. Multiple extended target tracking algorithm based on GM-PHD filter and spectral clustering. *EURASIP J. Adv. Signal Process.* **2014**, *2014*, 117. [[CrossRef](#)]
17. Dudczyk, J.; Rybak, Ł. Application of Data Particle Geometrical Divide Algorithms in the Process of Radar Signal Recognition. *Sensors* **2023**, *23*, 573–590. [[CrossRef](#)] [[PubMed](#)]
18. Qin, Z.; Kirubarajan, T.; Liang, Y. Application of an efficient graph-based partitioning algorithm for extended target tracking using GM-PHD filter. *IEEE Trans. Aerosp. Electron. Syst.* **2020**, *56*, 4451–4466. [[CrossRef](#)]
19. Ester, M.; Kriegel, H.P.; Sander, J.; Xu, X. A Density-Based Algorithm for Discovering Clusters in Large Spatial Databases with Noise. In Proceedings of the National Conferences on Artificial Intelligence, Orlando, FL, USA, 226–231 July 1996.
20. Granström, K.; Fatemi, M.; Svensson, L. Poisson multi-Bernoulli mixture conjugate prior for multiple extended target filtering. *IEEE Trans. Aerosp. Electron. Syst.* **2020**, *56*, 208–225. [[CrossRef](#)]
21. Granström, K.; Svensson, L.; Reuter, S.; Reuter, S.; Xia, Y.; Fatemi, M. Likelihood-Based Data Association for Extended Object Tracking Using Sampling Methods. *IEEE Trans. Intell. Veh.* **2020**, *56*, 208–225. [[CrossRef](#)]
22. Scheel, A.; Granström, K.; Meissner, D.; Reuter, S.; Dietmayer, K. Tracking and data segmentation using a GGIW filter with mixture clustering. In Proceedings of the 17th International Conference on Information Fusion (FUSION), Salamanca, Spain, 7–10 July 2014; pp. 1–8.
23. Hoffman, J.R.; Mahler, R.P.S. Multitarget Miss Distance via Optimal Assignment. *IEEE Trans. Syst. Man Cybern. Part A Syst. Humans* **2004**, *34*, 327–336. [[CrossRef](#)]
24. Ciunozzo, D.; Willett, P.K.; Bar-Shalom, Y. Tracking the Tracker from its Passive Sonar ML-PDA Estimates. *IEEE Trans. Aerosp. Electron. Syst.* **2014**, *50*, 573–590. [[CrossRef](#)]

Disclaimer/Publisher’s Note: The statements, opinions and data contained in all publications are solely those of the individual author(s) and contributor(s) and not of MDPI and/or the editor(s). MDPI and/or the editor(s) disclaim responsibility for any injury to people or property resulting from any ideas, methods, instructions or products referred to in the content.